International Journal of Advanced Science and Technology
Vol. 29, No. 7s, (2020), pp. 4725 - 4734

Parametric Modeling and Optimizing the Mechanical Properties of 3D Printed Recycled PLA Components

K. Devaki Devi[1*], M. Naga Phani Sastry[2], P. Venkateshwar Reddy[3]
[1, 2, 3]*Department of Mechanical Engineering, G. Pulla Reddy Engineering College, Kurnool, INDIA - 518007*

Abstract

Additive Manufacturing is occupying a significant role in the manufacturing of parts by giving an option in contrast to the current procedures. Anyway quality of such 3D printed parts utilizing explicit materials is as yet an area of current research. Polylactic acid, a biodegradable material, is one of the demanding materials in Fused Deposition Modeling based 3D printing process. The current work is centered on the investigation of the impact of the raster orientation and infill percentage on the mechanical properties of recycled poly Lactic Acid (PLA) printed parts. Samples were printed at three raster orientations (0°, 45°, 90°) and five infill percentages (20, 40, 60, 80, 100) to test impacts on part quality. This work considered the mechanical properties like tensile strength and flexural strength of 3D printed parts made with FDM innovation by shifting the infill and layer thickness parameters utilizing a statistical procedure RSM. ASTM D638 Type IV samples imprinted on FDM printer utilizing reused PLA material is exposed to tensile and flexural testing. Because of the layered creation process, 3D printed parts show anisotropic conduct. The outcomes demonstrated that the mechanical properties improve as the straight layer thickness parameter increments. The conduct was diverse in each test for the straight infill parameter.
Keywords: *PLA; Optimization; 3D printing; FDM; Mechanical Properties*

1. Introduction

Polylactic acid (PLA) is by a wide margin the most contemplated bio sourced feedstock material for polymer-based additive manufacturing [1–3]. PLA is gotten from starch by instruments of hydrolytic breaking and aging. The utilization of PLA in additive manufacturing fabricating procedures, for example, Fused Deposition Modeling (FDM) has numerous advantages. PLA displays a surprising capacity for thermo-framing under low preparing temperatures contrasted with other feedstock polymers. It has additionally quick crystallization after cooling. Other than the procedure capacity perspectives, PLA is biodegradable, inexhaustible asset, reasonable and shows a low harmfulness contrasted with ABS (acrylonitrile butadiene styrene) that is additionally generally utilized in FDM. The printing states of PLA have been broadly considered and these were identified with both the thermal and mechanical conduct of the crude polymer.

The thermal energy during printing particularly the resulting crystallization conduct of PLA is fundamentally influenced by its physicality and chemical arrangement. 3D printing is headway in printing innovation, able to convey many-sided shapes in a solitary piece from a CAD model. A .stl document is created from the CAD model and afterward exported to the 3D printing programming which delivers a genuine model in a layer by layer structure. FDM is an eccentric strategy with number of parameters that sway the material properties and nature of the item, and the blend of these parameters is difficult to comprehend. These printing parameters incorporate layer thickness, feed rate, infill design, thickness, raster width and edge, direction and so on which shows a critical impact on execution and prevalence of the 3D printed parts.

Lee et al. [4] examined the nature of 3D-printed PLA for a fluctuated air-cooling rate. It was indicated that this parameter affected fundamentally both the mechanical quality and the measurement precision. Liao et al. [5] explored the crystalline and porosity of 3D-printed PLA

utilizing X-ray diffraction. The authors demonstrated that distinctions were seen among thin and thick samples in view of various thermal narratives. While thin samples didn't concoct huge varieties, the thick ones uncovered diverse crystallization patterns relying upon the base temperature. Specifically, it was discovered that the nearness of δ crystallite structure (less steady than α structure) diminished the solidness of printed PLA.

Pandis et al. [6] detailed that the expansion in crystalline is found following a few days of in-administration for 3D-printed PLA. The creators ascribed this stage change to material maturing. As far as mechanical execution, tensile, compression, flexural, effect and fatigue conduct of PLA were corresponded to assortments of printing parameters, for example, the infill thickness, infill density, and printing direction to give some examples [7]. Chacon et al. [8] examined the impact of layer thickness on the mechanical presentation of 3D-printed PLA. The authors finished up on a differentiated impact of this parameter with respect to the part direction. The hugest impact was identified with the ductility decrease when the layer thickness was expanded. On account of the significance of the interfacial associations, a few examinations exhibit that post treatment of 3D-printed parts improves the mechanical presentation. For example, Shaffer et al. [9] revealed that improved interlayer attachment is gotten when the 3D-printed part is presented to ionizing radiation. This treatment adds to upgrade the polymer cross connecting.

Besides, Bhandari et al. [10] indicated that strengthening treatment with temperatures higher than the glass progress temperature improves between layer tensile strength. In light of certain issues identified with the utilization of unadulterated PLA in 3D printing, for example, absence of thermal solidness, fragility and degradation conduct, a few endeavors were made to mix the fiber with various materials, for example, lignin, hemp filaments, poly ε-caprolactone, wood flour and carbon whiskers, among different fillers.

2. Materials and Methods

FDM has a few preferences as for other manufacturing materials; there are a few issues that must be confronted. When setting the printing alternatives, a few parameters must be considered, for example, raster direction, temperature, speed, infill rate, and so forth. Choosing these parameters is regularly an extraordinary test for the user, and is commonly understood by understanding without thinking about the impact of varieties in the parameters on the mechanical properties of the printed parts. The current work is centered on the examination of the impact of the raster direction and infill rate on the mechanical properties of reused Poly Lactic Acid (PLA) printed parts. Example were printed at three raster direction edges (0°, 45°, 90°) and five infill rates (20, 40, 60, 80, 100) to test consequences for part quality. Optimum arrangement of parameters are gotten utilizing Response Surface Methodology to investigate the most extreme tensile and flexural properties. The PLA wire of 1.75 mm in diameter across has been fed into the nozzle.

2.1 3D printing of samples

PLA samples are printed utilizing CreatbotBot 3D Printer(Figure 1) that utilized Fused Deposition Modeling (FDM) innovation. The procedure conditions are: 0.4 mm for spout measurement, different raster angles, 0.2 mm for layer stature, with various infill, 150 mm/s for nozzle vertical speed, raft choice actuated, printing temperature shifted somewhere in the range of 210 and 255^{o}C. Raster oriented directions are shown in fig. 2. In spite of the fact that, the suggested printing temperatures for PLA are beneath 230^{o}C, the target of utilizing bigger temperatures is to evaluate the impact of huge temperature runs on mechanical execution that are not yet detailed. This permits to build up an increasingly exact parameter window for PLA printing.

Figure 1 3D printing machine setup

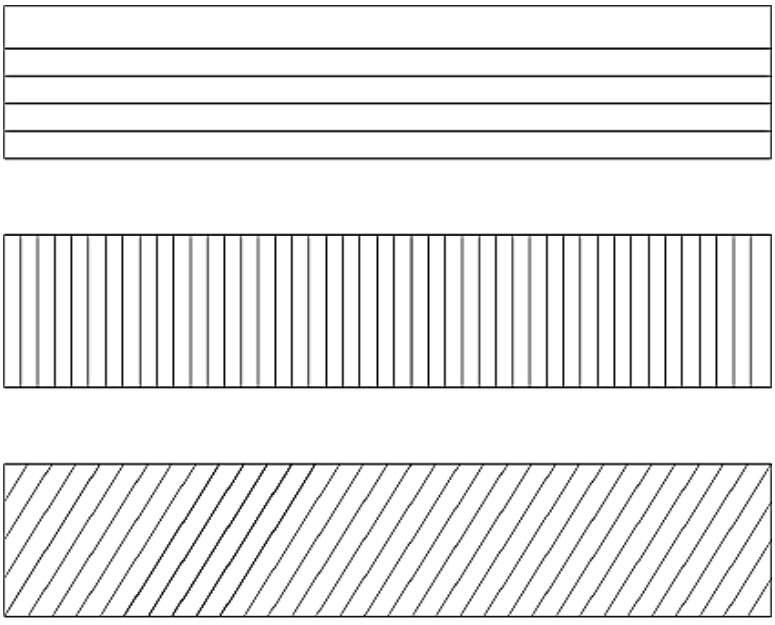

Figure 2 Raster orientation directions, 0° (top), 90° middle, and 45° (bottom)

2.2 Testing of samples

Tensile and flexural testing were conducted on 3D-printed PLA samples. Virgin PLA filaments were also subjected to tensile tests for comparison purpose. Mechanical characterization was performed utilizing Instron Universal Testing machine (Model-3369) with a load cell of 50 kN, and a fixed strain rate of 5 mm/min at a temperature of 30^{o}C with 50% relative humidity. Tensile testing and flexural testing samples dimensions are shown in figures 3 and 4 respectively.

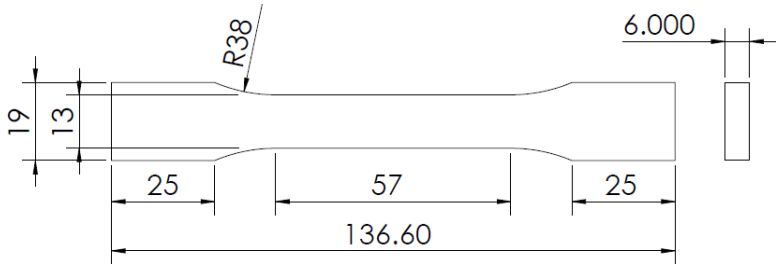

Figure 3 Tensile Specimen Dimensions in mm

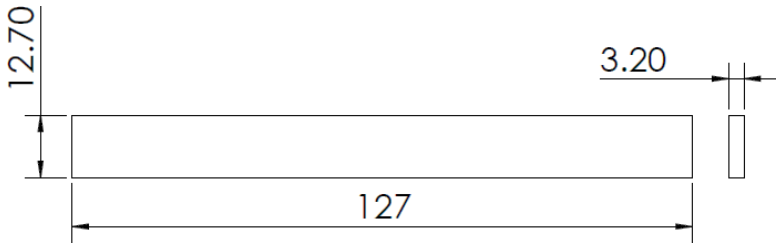

Figure 4 Bending Testing Specimen Dimensions

All printed material, including text, illustrations, and charts, must be kept within the parameters of the 8 15/16-inch (53.75 picas) column length and 5 15/16-inch (36 picas) column width. Please do not write or print outside of the column parameters. Margins are 3.3cm on the left side, 3.65cm on the right, 2.03cm on the top, and 3.05cmon the bottom. Paper orientation in all pages should be in portrait style.

3. Results and Discussion

3.1 Tensile test results

The 3D printed samples are tested for tensile properties with the proper specifications as mentioned in the previous section. The obtained results are tabulated in Table. 1.

Table 1 Tensile testing results of various 3D printed samples

Test No.	Raster Orientation (degrees)	Infill percentage	Ultimate Stress (MPa)	Elongation at Break (%)	Modulus of Elasticity (GPa)
1	0	60	59.65	2.198	3.256
2	0	20	58.61	2.297	2.815
3	0	40	54.16	1.697	3.522
4	0	80	65.49	2.271	3.461
5	0	100	54.36	1.656	3.599
6	45	80	64.94	2.552	3.677

7	45	20	63.28	2.368	3.577
8	45	60	62.45	2.413	3.598
9	45	40	65.37	2.577	3.585
10	45	100	64.10	2.601	3.585
11	90	40	56.26	5.086	3.507
12	90	60	56.08	3.208	3.536
13	90	100	53.34	4.530	3.463
14	90	20	49.10	4.553	3.310
15	90	80	55.26	3.334	3.628

From the table it is observed that the test number 4 obtained better tensile strength which contains a raster angle of 0^O and infill percentage of 80.

3.2 Flexural test results

The 3D printed samples are tested for flexural properties with the proper specifications as mentioned in the previous section. The obtained results are tabulated in Table. 2.

Table 2 Flexural testing results of various 3D printed samples

Test No.	**Raster Orientation (degrees)**	**Infill percentage**	**Ultimate Stress (MPa)**	**Elongation at Break (%)**	**Modulus of Elasticity (GPa)**
1	0	60	99.34	6.64	3.13
2	0	20	103.77	9.19	3.17
3	0	40	100.90	13.29	3.18
4	0	80	107.14	12.16	3.48
5	0	100	99.87	11.82	2.98
6	45	80	92.77	7.17	2.98
7	45	20	92.29	7.48	3.21
8	45	60	88.23	8.15	2.93
9	45	40	89.43	8.81	3.02
10	45	100	90.53	7.59	2.78
11	90	40	85.77	4.73	3.01
12	90	60	85.48	4.73	2.88
13	90	100	87.32	4.75	3.05
14	90	20	86.52	4.01	3.00
15	90	80	85.59	4.30	3.05

From the table 2 similar to the tensile test result, it is observed that the test number 4 obtained better flexural strength which contains a raster angle of 0^O and infill percentage of 80.

3.3 Tensile test on virgin PLA filament

Tensile testing on the virgin filament alone was also tested. Four displacement rates were used to test the filament. Table 3 shows a summary of the results for each strain rate.

Table 3 Summary of virgin filament tensile testing

Displacement Rate (mm/min)	Average Ultimate Stress (MPa)	Ultimate Strain (%)	Modulus of Elasticity (GPa)
500	58.951	9.2%	1.778
200	59.518	13.3%	1.868
50	54.713	17.5%	1.636
5	48.233	16.0%	1.309

For the two fastest strain rates (500 mm/min and 200 mm/min) the ultimate stress was similar along with the modulus of elasticity. The two slower strain rates (50 mm/min and 5 mm/min) had lower ultimate strengths, but did have higher elongations before failure – likely affected by creep from the longer testing times. The ultimate stress for the faster strain rates (not affected by creep) was similar to the results of the printed specimen, even though the PLA plastic in the specimen has been heated and extruded one time more than the filament alone. This finding clarifies that recycled PLA filaments can be printed with satisfactory results.

4. Modeling and optimization of process parameters

In the greater part of the introduced explore, the optimum mix of procedure parameters was resolved from a test study, and the exploratory result that produced a superior arrangement was considered as the optimal arrangement. In any case, the blend of process parameters for the best arrangement might be not quite the same as the experimental combinations, and they should be inside the permissible scope of procedure parameters. To defeat this inadequacy, diverse advancement strategies were utilized by various researchers.

In most optimization issues, the objective function is a scientific model that speaks to the connection between process parameters and one single part's trademark. In multi-target enhancement, a mix of mathematical models is utilized to speak to the connection between process parameters and various parts' attributes. The requirements are the admissible scope of procedure parameters; by and large, this speaks to the most elevated and least degrees of procedure parameters from the FDM machine or a scope of procedure parameters that are known to create great part qualities. In the current work, exploratory design is broke down and optimal parameters are obtained utilizing response surface methodology.

4.1 Response surface methodology

Response surface methodology is an assortment of scientific and statistical methods that are utilized for demonstrating and examination of issues in which yield or reaction impacted by number of factors and the goal is to discover the connection between's them. It is an observational displaying strategy, committed for assessment of relations existing between a gathering of controlled test factors and the watched consequences of at least one chose standards. Earlier information on the examined procedure is along these lines important to manufacture a reasonable model.

The initial step of RSM is to characterize the constraints of the trial area to be investigated. These cutoff points are made as wide as conceivable to get a clear response from the model. The optimal structure gives similarly an exact expectation of all reaction variable midpoints identified with amounts estimated during experimentation. Optimal design offers the bit of leeway that specific scope of alterations is permitted and can be utilized in two-advance sequential response surface methods. In these techniques, there is a likelihood that the analyses will stop with genuinely hardly any runs and conclude that the forecast model is agreeable. The conduct of the framework is clarified by the accompanying observational second-order polynomial model.

$$\textbf{Response} = b_o + b_aA + b_bB + b_{aa}A^2 + b_{bb}B^2 + b_{ab}AB \quad (1)$$

A scientific model of a response surface gives more data on the grounds that envisioning the response surface's shape will be made conceivable. To fabricate the model, estimations of the response for a scope of factor levels are gathered and afterward numerical model of the response surface is assembled. There are two normal sorts of models, the hypothetical models, wherein the hidden hypothetical connection between the response and the components is very much characterized and the observational models, wherein the least complex polynomial condition is tried, that sufficiently prove the information. Analysis of variance (ANOVA) for the ampleness of the model is then acted in the resulting step. The F proportion and p-value are determined for 95% degree of certainty. The variables with p-value under 0.05 are viewed as noteworthy and those more prominent than 0.05 are irrelevant. The ANOVA of tensile modulus and flexural modulus are shown in table 4 and table 5 respectively.

Table 4 ANOVA for Tensile Modulus (M)

Source	Sum of Squares	df	Mean Square	F-value	p-value	
Model	0.4371	5	0.0874	3.74	0.0414	significant
A-RO	0.1001	1	0.1001	4.28	0.0684	
B-IP	0.1852	1	0.1852	7.93	0.0202	
AB	0.0583	1	0.0583	2.50	0.1486	
A^2	0.1264	1	0.1264	5.41	0.0451	
B^2	0.0509	1	0.0509	2.18	0.1741	
Residual	0.2103	9	0.0234			
Cor Total	0.6474	14				

Form the above ANOVA Table, it can be observed that the Model F-value of 3.74 implies the model is significant. P-values less than 0.0500 indicate model terms are significant. In this case IP, RO^2 are significant model terms. The predicted model is given as:

$$M = 2.72073 + 0.0140111 * RO + 0.0165462 * IP - 0.00006 * RO * IP - 0.0000961481 * RO^2 - 0.0000870238 * IP^2 \quad (2)$$

Table 5 ANOVA for Flexural Modulus (F)

Source	Sum of Squares	Df	Mean Square	F-value	p-value	
Model	0.1740	3	0.0580	38.68	<0.0001	significant
A-RO	0.1706	1	0.1706	113.77	<0.0001	
B-IP	0.0027	1	0.0027	1.82	0.2046	

AB	0.0128	1	0.0128	8.51	0.0140	
Residual	0.0165	11	0.0015			
Cor Total	0.1905	14				

The Model F-value of 38.68 implies the model is significant. P-values less than 0.0500 indicate model terms are significant. In this case RO, RO*IP are significant model terms. The predicted model is given as:

$$F = 3.26585-0.004481*RO-0.001739*IP+0.000028*RO*IP \quad (3)$$

Optimal solution has been derived for the specified design space constraints for individual response characteristics viz. raster orientation and infill percentage using Design Expert V-11.0 statistical software. Table 4 reports the optimal set of conditions with higher desirability required for obtaining the best possible response characteristics.

Table 6 Optimal Solution Set

Raster Orientation-RO (^{0})	**Infill Percentage-IP (%)**	**Modulus of Elasticity-E (GPa)**	**Flexural Modulus-F (G Pa)**	**Desirability**
17.156	70.411	3.594	3.100	0.824

From the above table, maximum tensile and flexural strengths can be obtained when the component or specimen is printed at (≈)17^0 with 70.4% infill density, which is likely to be feasible evident from desirability factor. The optimum results are graphically represented in the figures 5 to 7 with the help of ramped and 3D plots respectively.

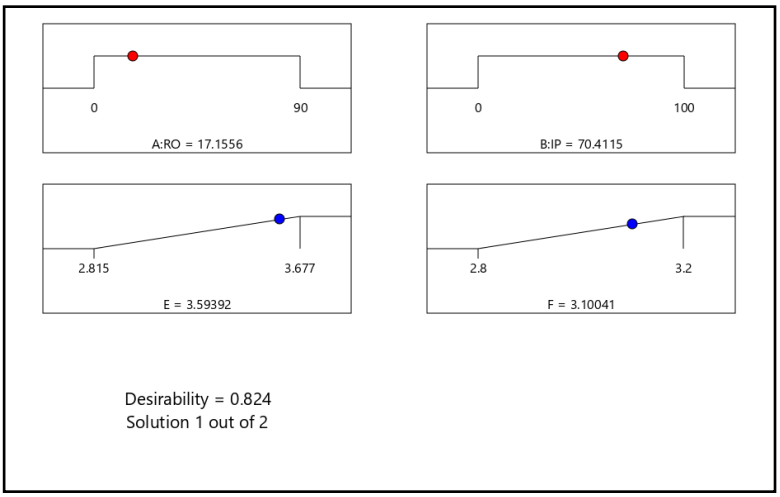

Figure 5 Ramped Plots for Optimum Values

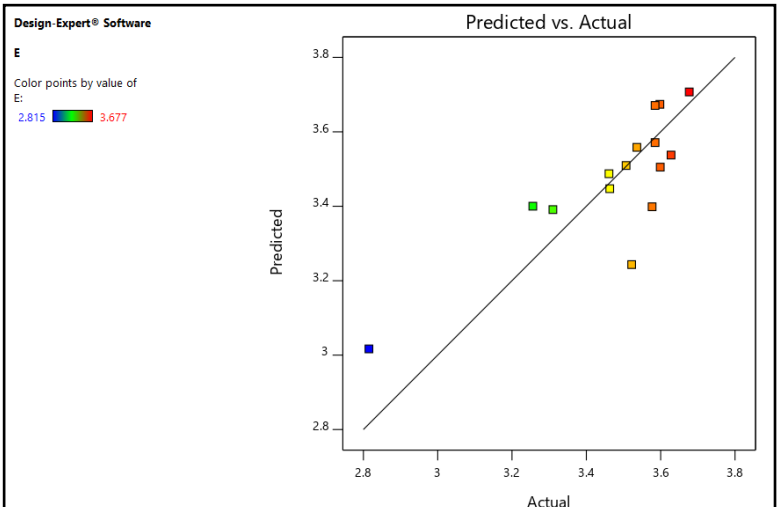

Figure 6 Predicted Vs Actual plot for Modulus of Elasticity

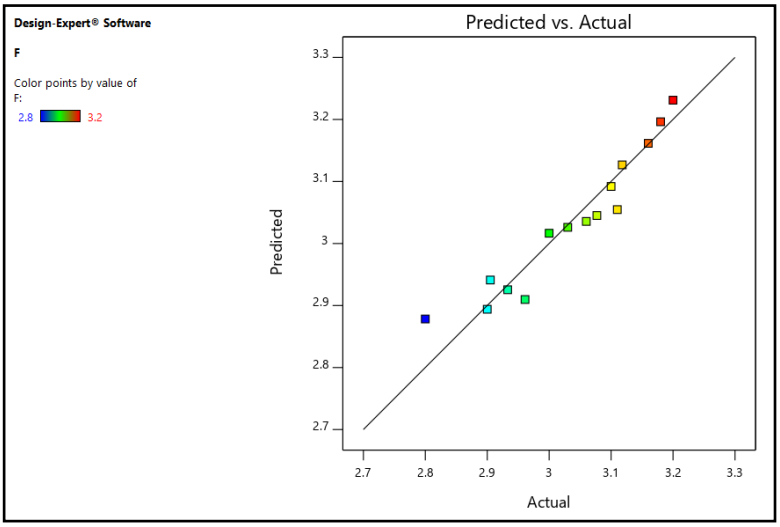

Figure 7 Predicted Vs Actual plot for Flexural Modulus

Conclusions

- PLA printed and specimen PLA filament mechanical properties were tested. For both tensile and flexural testing, it was experimentally determined that the 0° raster orientation specimens were observed to be strongest.
- From the response surface analysis, maximum tensile and flexural strengths can be obtained when the component or specimen is printed at (≈) 17^0 raster orientation with 70.4% infill density.
- It is also evident that single recycled PLA filaments are feasible for 3D printing with satisfactory output.

References

1. Abouzaid, K., Guessasma, S., Belhabib, S., Bassir, D., & Chouaf, A. (2018). Printability of co-polyester using fused deposition modelling and related mechanical performance. *European Polymer Journal*, *108*, 262-273.
2. Ahn, S. H., Montero, M., Odell, D., Roundy, S., & Wright, P. K. (2002). Anisotropic material properties of fused deposition modeling ABS. *Rapid prototyping journal*.
3. Aliheidari, N., Tripuraneni, R., Ameli, A., & Nadimpalli, S. (2017). Fracture resistance measurement of fused deposition modeling 3D printed polymers. *Polymer Testing*, *60*, 94-101.
4. Lee, C. Y., & Liu, C. Y. (2019). The influence of forced-air cooling on a 3D printed PLA part manufactured by fused filament fabrication. *Additive Manufacturing*, *25*, 196-203.
5. Liao, Y., Liu, C., Coppola, B., Barra, G., Di Maio, L., Incarnato, L., & Lafdi, K. (2019). Effect of porosity and crystallinity on 3D printed PLA properties. *Polymers*, *11*(9), 1487.
6. Pandis, P. K., Papaioannou, S., Koukou, M. K., Vrachopoulos, M. G., & Stathopoulos, V. N. (2019). Differential scanning calorimetry based evaluation of 3D printed PLA for phase change materials encapsulation or as container material of heat storage tanks. *Energy Procedia*, *161*, 429-437.
7. Casavola, C., Cazzato, A., Moramarco, V., & Pappalettere, C. (2016). Orthotropic mechanical properties of fused deposition modelling parts described by classical laminate theory. *Materials & design*, *90*, 453-458.
8. Chacón, J. M., Caminero, M. A., García-Plaza, E., & Núñez, P. J. (2017). Additive manufacturing of PLA structures using fused deposition modelling: Effect of process parameters on mechanical properties and their optimal selection. *Materials & Design*, *124*, 143-157.
9. Shaffer, S., Yang, K., Vargas, J., Di Prima, M. A., & Voit, W. (2014). On reducing anisotropy in 3D printed polymers via ionizing radiation. *Polymer*, *55*(23), 5969-5979.
10. Bhandari, S., Lopez-Anido, R. A., & Gardner, D. J. (2019). Enhancing the interlayer tensile strength of 3D printed short carbon fiber reinforced PETG and PLA composites via annealing. *Additive Manufacturing*, *30*, 100922.